Supporting information

Sensitization of nickel oxide: improved carrier lifetime and charge collection by tuning nanoscale crystallinity

Xiao Li Zhang,*[a] Zhipan Zhang,*[b] Dehong Chen,[c] Peter Bäuerle,[d] Udo Bach[e] and Yi-Bing Cheng[e]

[a]*School of Chemical Engineering, the University of New South Wales, Sydney 2052, Australia.*
E-mail: xiaolizhang.z@gmail.com;
[b]*Key Laboratory of Cluster Science, Ministry of Education of China, School of Chemistry, Beijing Institute of Technology, Beijing, China.*
E-mail: deanzhang1980@gmail.com.
[c]*Department of Chemistry, the University of Melbourne, Melbourne 3001, Australia.*
[d]*Institute for Organic Chemistry II and Advanced Materials, University of Ulm, Albert-Einstein-Allee 11, 89081 Ulm, Germany.*
[e]*Department of Materials Engineering, Monash University, Melbourne 3800, Australia.*

Experiments

Fabrication of p-DSCs: NiO nanoparticles (particle size ~20 nm, 99.9%, Inframat Advanced Materials) were ball-milled in ethanol with few droplets of acetate additive for 2 hrs. The mixture of above colloidal solution, ethyl cellulose (Aldrich) and terpinol anhydrous (≥99.5%, Fluka) were sonicated and stirred alternatively to obtain a fine dispersion. A paste was made by evaporating the ethanol from the mixture on a rotary evaporator. FTO glass (Nippon sheet glass, resistance 13 Ω/square) were coated with nickel acetate (+98%, Alfa Aesar) ethanol (≥99.7%, Merck) solution (0.05 M) by dip-coating and subsequently dried before screen print. The photocathode films were screen-printed with the NiO paste and dried for 5 min at 125 ºC. This coating-drying procedure was repeated to obtain films with different thickness. The NiO electrodes were sintered under an air flow at 450 ^{o}C for 30 min with a ramping time of 30 min from room temperature (~25 ^{o}C) to 450 ^{o}C, and then post-treated at 550 ^{o}C for 15 min with a ramping time of 10 min from 450 ^{o}C to 550 ^{o}C. Average device results suggest that 15 minute is the optimized treatment time at 550 oC to significantly improve the photovoltage without losing much surface area of NiO nanocrystalline films for efficient dye loading. After cooling to room temperature, the electrode films were soaked in a 0.2 mM dye solution overnight. The resulting NiO working electrodes were assembled and sealed with the counter electrodes made by sputtering coating Pt on FTO glass to produce a sandwich type cell. The electrolyte, containing 0.03 M iodine, 0.5 M 4-terbutylpyridine, 0.6 M 1-butyl-3-methylimidazolium iodide, and 0.1 M guanidinium thiocyanate in a mixed acetonitrile and valeronitrile (with volume ratio of 85 : 15) solution, was introduced into the cell via a vacuum filling method.

Characterization: Morphology observation and crystal structure of NiO nanorods were verified by Transmission Electron Microscope (FEI Tecnai G2 20 TEM) and X-ray Powder Diffraction (Phillips powder diffractometer). Brunauer – Emmett – Teller (BET) analysis based on N_2 adsorption has been used to determine surface area and the pore size distribution using the Barrett – Joyner – Halenda (BJH) method on a TriStar II 3020 Surface Area and Porosity Analyzer. The thickness of the NiO films was measured by using a profilometer (DEKTAK 150, Veeco Instruments Inc). The reflection spectra at wavelength range of 300–800 nm of mesoporous NiO were collected by using a Cary 5000 ultra-violet–visible - near-infrared (UV-Vis-NIR) spectrophotometer equipped with an integrating sphere (Internal DRA-2500).

The sealed solar cells were shielded by a black metal mask with an aperture area of 0.36 cm^2, and measured the photovoltaic properties using a Keithley 2400 Source Meter under the irradiation of simulated sunlight (100 mW/cm^2) provided by an Oriel solar simulator with an AM 1.5 filter. IPCE plotted as a function of excitation wavelength was recorded on a Keithley 2400 Source Meter under the irradiation of a 300 W xenon lamp with an Oriel Cornerstone^{TM} 2601/4m monochromator. Electrochemical impedance spectroscopy (EIS) was measured with an AutoLab PST A30 in a frequency range of 0.1 – 10^5 Hz under 1 sun of AM1.5 simulated solar radiation and an applied electrical bias dropping from the open-circuit voltage (V_{oc}) of the device to 100 mV below V_{oc} with a 20 mV interval. EIS spectra were then fitted in Zview software with a transmission line model shown in Figure S7. Generally, an EIS spectrum of a DSC comprises three distinctive parts associated with electrochemical processes of different time domains, i.e. the fast response from charge transfer at counter electrode in the high frequency domain, the signal from carrier transport and recombination in the semiconductor layer in the mid-frequency domain and the slow response from the Nerstain diffusion of redox couple species in the electrolyte taking place in the low frequency domain. Depending on the characteristic time constants of the individual processes, responses from one or more processes would dominate the EIS spectrum and provide pertinent information of the whole device. See a case discussion in Figure S6.

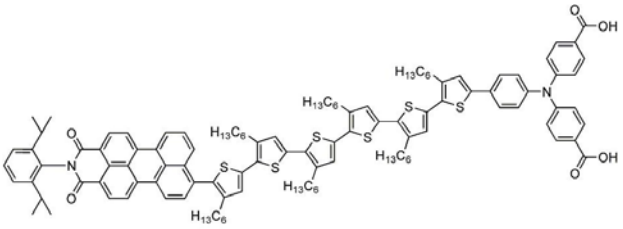

Figure S1. Chemical structure of dye. The chemical structure of the p-type dye contained an oligothiophene coupled to triphenylamine as the donor and a perylenemonoimid as the acceptor.

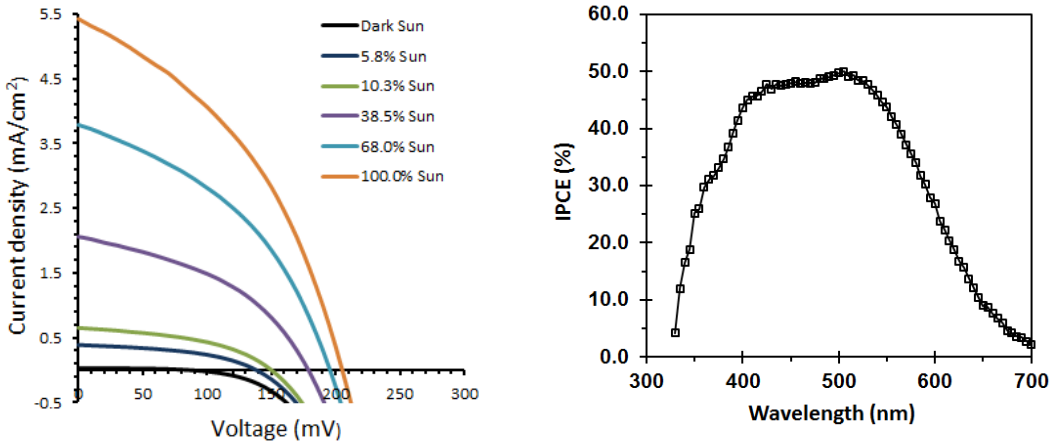

Figure S2. Photocurrent density – voltage characteristics under simulated AM 1.5G illumination at different light intensity and incident photon to current conversion efficiency (IPCE) characteristics of *p*-type DSC prepared from NiO nanocrystalline films without post-treatment at 550 ^{o}C. 100% sun corresponds to 100 mW cm^{-2}.

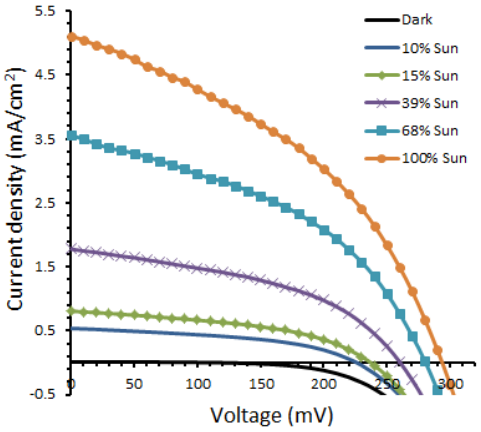

Figure S3. Photocurrent density – voltage characteristics under simulated AM 1.5G illumination at different light intensity of *p*-type DSC prepared from NiO nanocrystalline films with post-treatment at 550 ^{o}C. 100% sun corresponds to 100 mW cm^{-2}.

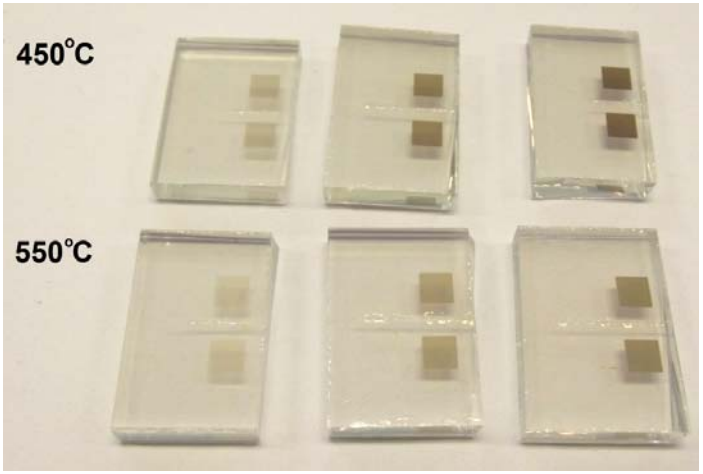

Figure S4. NiO films with a variety of film thickness of 1.1, 2.2 and 3.2 μm prepared at 450 °C and with a post-treatment at 550°C.

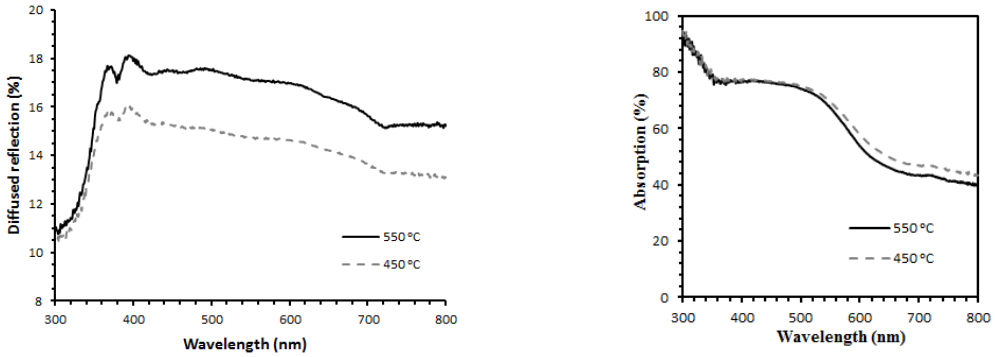

Figure S5. Diffuse reflectance spectra of mesoporous NiO films (left) and UV-vis absorption spectra of dyed NiO films (right) prepared at 450 °C and with a post-treatment at 550°C.

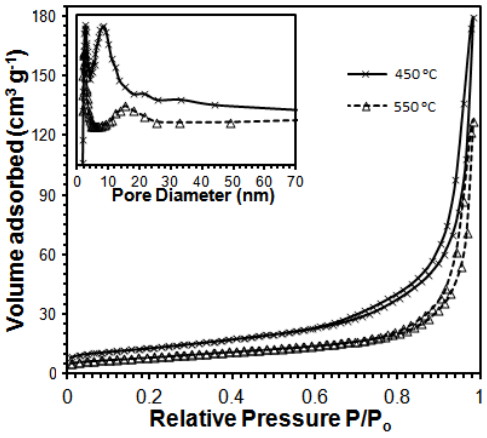

Figure S6. BET analysis of mesoporous NiO after sintered at 450 and with post-treatment at 550 °C. Based on BET measurement, the post-treatment brought an approximately 38% decrease in the specific surface area of the mesoporous NiO film from 55 $m^2 g^{-1}$ to 34 $m^2 g^{-1}$and broadened the major pore size from 8.5 nm to 15.3 nm.

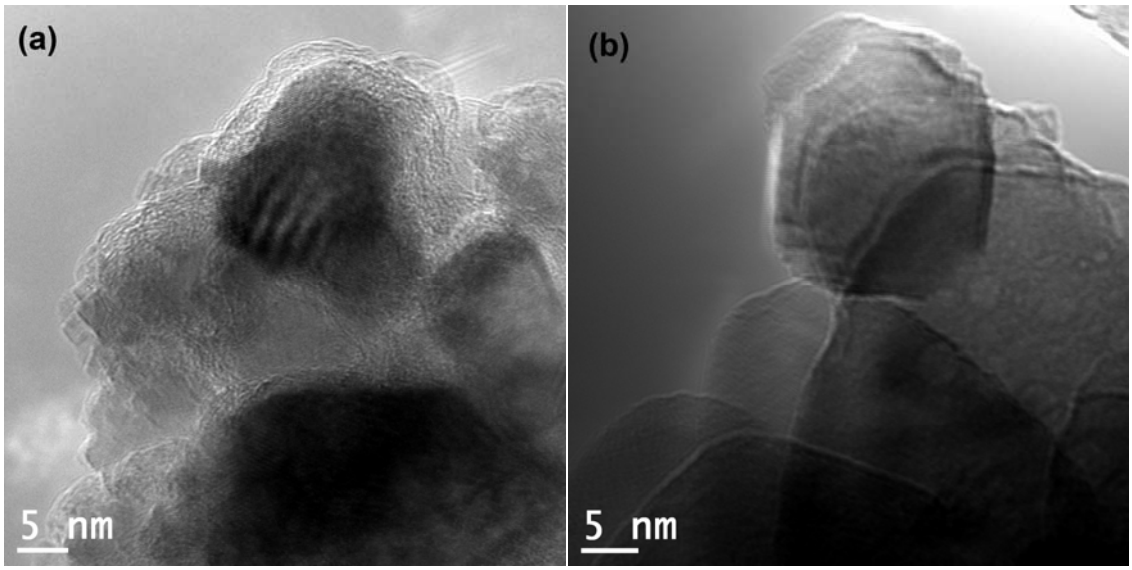

Figure S7. HRTEM images of NiO nanoparticle (a) after sintered at 450 and (b) with post-treatment at 550 °C. Before the post-treatment, an amorphous shell can be easily found on many NiO nanoparticles, while the post-treatment fosters the formation of clear lattice fringes at the edge of the nanoparticle and confirms the well-developed nanoscale crystallinity.

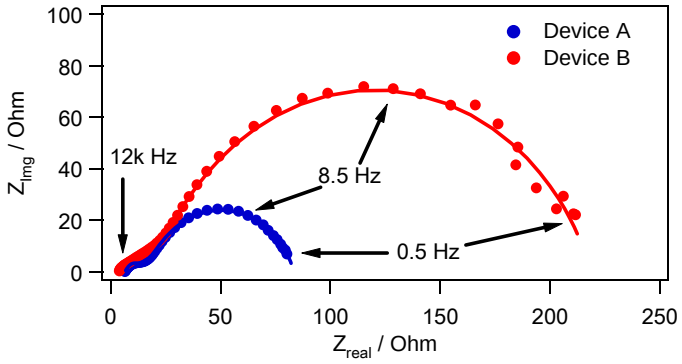

Figure S8. Typical EIS spectra of two devices made of NiO photocathode without (Device A) and with (Device B) 550 °C post-treatment. The devices were measured at 0.22 V bias under the AM 1.5G illumination at 100 mW cm^{-2} (1 sun). In the current case, the response from counter electrode in the high frequency region is overshadowed by the large impedance of hole diffusion in the NiO film in both spectra and particularly indiscernible in the spectrum from Device B. While both spectra show a distinct semicircle in the mid-frequency region, implying a large enough charge transfer resistance at the NiO/electrolyte interface, the EIS spectrum of Device A features a stronger Warburg diffusion due to the slow transport of holes in NiO mesoporous layer and suggests a hole diffusion length (L_h) comparable to the film thickness, d, at this bias and light intensity. Wang et al. has shown that reliable values of charge transfer resistance at the semiconductor/electrolyte interface (R_{ct}) and the resistance to the carrier transport in the semiconductor layer (R_{tr}) could still be reliably obtained by fitting the EIS spectra with a transmission line model if the electron diffusion length, L_n, satisfies $L_n \geq d/2$.[1]

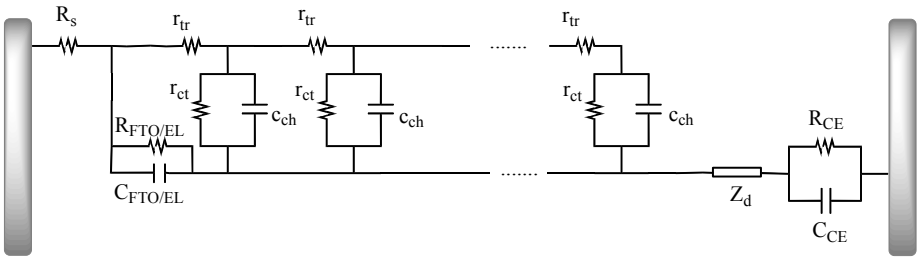

Figure S9. Equivalent circuit for fitting EIS spectra of *p*-DSCs. *R*s represents the serial resistance of the device, Z_d is the Warburg impedance due to the electrolyte diffusion, while R_{CE} and C_{CE} are the charge transfer resistance and the double layer capacitance of the platinized counter electrode, respectively. $R_{FTO/EL}$ and $C_{FTO/EL}$ stand for the charge transfer resistance and the corresponding double layer capacitance at exposed FTO/electrolyte interface. Processes of hole transport in the NiO and recombination with the I^- are depicted by the distributed element in the middle of the circuit, where r_{tr}, r_{ct} and c_{ch} are local resistance for hole transport, charge transfer resistance at the NiO/electrolyte interface for hole recombination with I^- and the distributed capacitance of NiO particles. Taking d as the thickness of the NiO film, the total hole transport resistance is R_t =

$r_{tr} \times d$ and the total interfacial charge recombination resistance is $R_{ct} = r_{ct} / d$. The lifetime and apparent diffusion coefficient of holes in the NiO film can be calculated.

Reference to Supporting Information

[1] J.R. Jennings, F. Li, Q. Wang, *J. Phys. Chem. C* 2010, **114**, 14665.